



# Investigation on the design of a novel selective laser melted insert for extrusion dies with conformal cooling channels

B. Reggiani<sup>1</sup> · I. Todaro<sup>2</sup>

Received: 21 January 2019 / Accepted: 16 May 2019 / Published online: 10 June 2019  
© Springer-Verlag London Ltd., part of Springer Nature 2019

## Abstract

The thermal control and the maintenance of a uniform temperature in the extrusion process of aluminum alloys is a crucial task in order to generate sound profiles with high press productivities. This can be accomplished through liquid nitrogen flowing in Conformal Cooling Channels (CCC). The Selective Laser Melting (SLM) additive technology offers an optimal solution for an unlimited flexibility of the cooling system, thus allowing tailored cooling strategies. In the present work, a smart thermally controlled die made by AISI H13 was designed aimed at maximizing and regulating the cooling efficiency by means of CCC. In the novel die concept, the expensive SLM insert with CC channels, has been integrated into a conventionally machined steel housing. A comprehensive numerical investigation has been performed in order to check the insert designs mechanical and thermal performances both in uncooled and cooled conditions. Then, eight inserts were additively manufactured by means of the SLM process with the aim to preliminary verify their experimental feasibility and overall quality. As main results, it was numerically proved the capability of the novel insert design to allow a significantly increase of the production rate and it was experimentally demonstrated the insert manufacturability throughout the SLM technology.

**Keywords** extrusion · Nitrogen cooling · Finite element modelling · Additive manufacturing · Selective laser melting (SLM)

## 1 Introduction

Guarda tu se sostituire la roba sottolineata (originale) con la roba in grassetto.

Extrusion of aluminum alloys is a consolidated process with relatively high efficiency and high market share. The speed of the extrusion and the exit profile temperature directly affect the process efficiency and their monitoring and control should be considered a crucial activity in order to produce defect-free profiles and maximize the overall productivity. During each billet extrusion, the temperature in the die, as well as in the exit profile, significantly increases due to the amount of work spent to plastically deform the billet and to overcome

friction at the tools/billet interfaces that is converted into heat [1]. Furthermore, the level of the achieved temperature increases not only with the extrusion ratio but in particular with the ram speed leading to potential surface defects, such as profile thinning, tearings or hot cracks [2–4]. Despite its drawbacks, the ram speed represents the main control parameter to guarantee high process productivity so that optimal working conditions have to be identified in order to achieve the dual aim of sound products and high production rates. In the last years, many extruders recognized the importance of the process thermal field evolution and monitoring thus proceeding to install pyrometers on the presses for the contactless monitoring of the temperatures along the whole production chain in order to obtain the so called ‘isothermal extrusion’ [5]. Benefits associated with the maintenance of a uniform temperature are related to a metallurgical uniformity (grain size, precipitate dissolution and longitudinal weld quality in hollows profiles), uniform mechanical properties of the profile, surface quality and optimal press productivity [6].

A detailed analysis of the data acquired by pyrometers proved, as previously stated, a strong connection between the appearance of profile defects and an excessive achieved temperature, thus requiring a reduction of the ram speed and

---

✉ B. Reggiani  
barbara.reggiani@unimore.it

<sup>1</sup> DISMI Department of Sciences and Methods for Engineering, University of Modena and Reggio Emilia, Via Amendola 2, 42122 Reggio Emilia, Italy

<sup>2</sup> DIN Department of Industrial Engineering, University of Bologna, Viale Risorgimento 2, 40136 Bologna, Italy

consequently limited production rates. In order to overcome these limitations, some options are nowadays practiced at industrial level. One option is the already cited isothermal extrusion in which the profile exit temperature is aimed at constant value during the whole production batch, i.e., for the whole billet length and the whole charge. This is accomplished by an optimization of the temperatures (different zones of the container and billet taper) and a retroacted control of the ram speed that is increased or decreased as a function of the temperature monitored by the pyrometer on the profile. However, this involves a deep understanding of the mechanics and thermodynamics of extrusion [1] and generally leads to a reduction of the global process productivity. Moreover, in many practical cases, extruders act on single parameters like the reduction of billet pre-heating temperature or by making use of tapered billets without a real global optimization of the process. As a consequence, this solution implies higher press loads and then higher stresses for the tooling set, not compensated by the low marginal increase of the allowed ram speed [7].

A further option is to remove the excess of temperature in the die ‘as near as possible’ to the bearing, where the profile is subjected to severe strains and heavy friction thus creating the highest temperature of the aluminum in the whole extrusion path [8]. In this context, a number of systems for die cooling through gas or liquid nitrogen have been mounted in the last decades on extrusion plants. Many companies thus re-evaluated the die cooling systems, in particular those using gas or liquid nitrogen that represents a cheap and safe source of cold. To date the heat removal is applied far away from the bearings; indeed cooling channels are usually industrially implemented by adding another element in the tooling set usually called ‘third plate’. Third plate is an element in between the die and the bolster. In the mating section between the die and the third plate channels for nitrogen flows are simply milled, then holes are drilled in order to evacuate the nitrogen towards the profile surface [9]. This should grant the double advantage of reducing the tooling set and profile exit temperatures and to inhibit the profile surface oxidation by creating an inert atmosphere owing to the gaseous nitrogen exiting the channels [10]. This manufacturing strategy, although quite simple, realizes cooling channels far away from bearings (usually more than 30/50 mm) and it also strongly limits channel geometry design. Nevertheless, today all majors and advanced extruders have already implemented liquid nitrogen cooling systems in order to increment their competitiveness and the installation in existing plant is growing.

However, the literature is still poor of studies on the nitrogen effect and involved parameters optimization. Ward et al. [10] experimentally investigated a number of solid and hollow profiles demonstrating the liquid nitrogen capability to increase productions rate and profile surface quality. Stratton et al. [11] proved that the gain achievable by the use of liquid

nitrogen is very dependent on the profile being extruded and on the die design. However, the extrusion speed and the die life were increased over 100% and up to 200% respectively by adopting a nitrogen cooling. Donati et al. [9] tested the effects of different nitrogen flows on the evolution of the die and profile exit temperature and on the process load for a complex industrial hollow profile made of AA6060. As main output it was found that the effect of nitrogen cooling on die temperature can be from irrelevant to extreme, in relation to the distance of nitrogen inlet. More recently, Ciuffini et al. [12] compared the surface quality of both nitrogen cooled and classically extruded products highlighting a strong improvement whenever the die was cooled.

An efficient solution to realize a more effective cooling action is the use of conformal cooling channels (CCC), i.e., channels that follow the bearing and tool shapes having a general high level of geometrical complexity. The CC channels can be located around the bearing in order to provide a relevant cooling flow exactly where the highest amount of heat is generated, i.e., the bearings. The complexity of application of CC channels is in their manufacturing: subtractive technologies are not able to realize the required geometry complexities of such designs. On the other side, recently developed additive technologies reduce the manufacturing effort and overcome the main drawbacks while increasing the design freedom of the cooling system. Additive manufacturing (AM) offers virtually unlimited flexibility of channel shape and aspect ratio, thus allowing tailored cooling strategies to induce a homogeneous temperature map in the die around the profile. The manufacturing peculiarities of the AM technologies perfectly fits with the requirement of dies, tools and inserts in terms of both batch sizes and freedom of design. Indeed, usually, a limited number of tools are required to be manufactured for the same profile geometry and the lack of design constraints allows to easily produce efficient CCC.

A number of works in literature reported the application of CCC generated by the use of AM technologies in different manufacturing processes. In polymer injection moulding, tools integrate CCC in order to reduce the cooling time of a 20–50%, to avoid hot spots and to increase production quality and efficiency [13–15]. Conformal cooling channels are also adopted for blow moulding of hollow-shaped parts in which the unforced cooling time usually takes 70% of the total production time [16]. Others manufacturing segments involving the use of CCC as strategical approach to increase the production rates or decrease the product defects are represented by press hardening (hot stamping or hot sheet metal forming) [17] and die casting applications [17–19]. Moving in the context of bulk metal forming, to the best of the author’s knowledge, to date only few works have been published on the manufacturing of extrusion dies with CCC by means of AM technologies. In detail, Holker et al. [8, 20] tested the effect of a temporary applied die cooling with compressed air in the

production of a hollow profile, resulting in a reduction of the extruded exit temperature of around 30 °C. Then, the same authors [21] introduced the further novelty of isolating the feeding of the coolant up to the die bearings where the cooling shall be localized. Among the many AM technologies, Selective Laser Melting (SLM) is a powder bed technology that built up solid parts layer by layer by means of a laser scanning that sequentially melt the powder material under an inert atmosphere. SLM has been proved to be able to process and completely melt to an almost 100% dense microstructure standard high-alloy tooling materials such as the H13 traditionally used to manufactured extrusion dies [22–25].

Cost considerations needs a special attention when talking about AM technologies since raw material (high quality powders) is much more expensive than conventional bulk metal and AM technologies have limits in terms of product dimensions and hourly costs. The idea of realizing full AM dies is today far away from costs remuneration. Nevertheless if a mixture of conventional die and AM inserts to be locked inside the die can be applied, the costs of the additive part can be substantially reduced down to a level acceptable by the market.

In such situation die makers will have to face new challenges: how to design an efficient conformal cooling channel? How to guarantee the resistance of the die, in particular when a tool composed by die plus insert have to be manufactured? How to preliminary validate the cooled die functionality without expensive trial-and-error experimental procedures? Indeed, if FE simulations are receiving an increased attention as supporting tools for conventional die design [26–32], with CCC dies their use become mandatory. Nevertheless, even if the FE modelling of cooling channels has been reported in literature for plastic injection moulding and die casting applications [14, 19], to the best of the author's knowledge, in the field of the extrusion process, only a few works have been carried out in terms of numerical assessment on the impact of cooling channels in controlling the die and the profile exit temperature [8]. In addition, a consistent part of the published

work adopted water as cooling media or used simplified convective coefficients applied to channel walls [33].

In the present work, with the aim to further push the novel concept design towards the industrial attention in the extrusion framework, a smart thermally controlled die made by AISI H13 was designed aimed at maximizing and regulating the cooling efficiency by means of CCC. In the novel die concept, the expensive selective laser melted insert with CC channels has been integrated into a steel housing conventionally machined. In order to check and verify the insert functionality, a comprehensive numerical analysis has been performed on the final selected insert designs before their manufacturing based on a novel FE model of the extrusion process coupled with nitrogen cooling.

## 2 Insert concept design

The novel extrusion tool has been thought as composed of two parts, both made by standard hot work tool steel AISI H-13. A first part was the insert with conformal cooling channels (CCC) to be manufactured by the selective laser melting process and the second part was the tool steel housing made by conventional machining. Concerning the insert with CCC, a preliminary design stage has been performed. A profile produced in a relevant amount, with a short die lifetime and critical issues on thermal field has been identified and selected. It was a round solid bar of 10 mm diameter usually produced with both aluminum alloy AA6060 and magnesium alloy ZM21. At the design stage, a helical conformal cooling channel for liquid nitrogen have been selected since properly embracing the working zones of the insert for the selected bar profile. The definition of the helical channel geometry was taken thoroughly into account in order to grant the full insert thermal performance. Helix pitch and channel diameter had to be the best trade-off among liquid nitrogen flow capability, nitrogen inlet and outlet channels position and mechanical

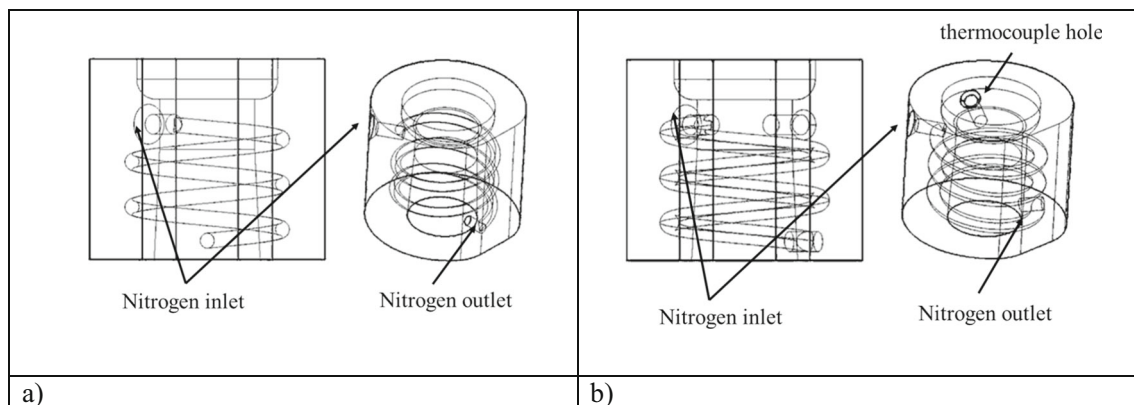


**Fig. 1** **a** Details of the first draft of the insert with helical CCC (extrusion direction top–bottom). **b** evolution of the insert design with a 1.5-mm diameter of the channel

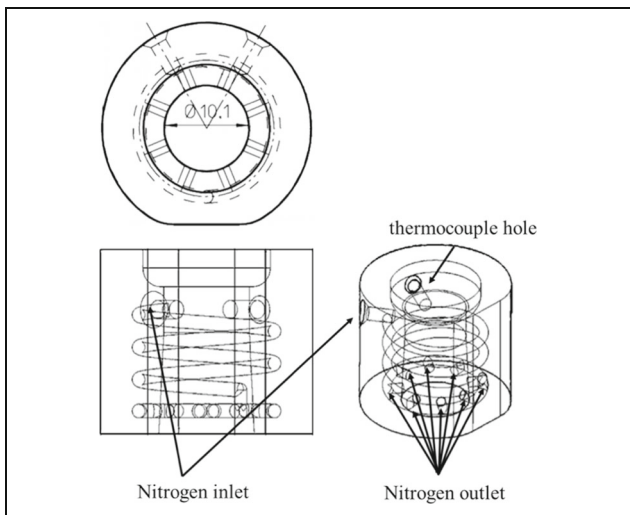


**Fig. 2** Third evolution stage of the insert design (extrusion direction top-bottom)

resistance of the insert. The geometry optimization accounted also for the constraints imposed by the thermocouple hole position that had to be contemplated in order to experimentally assess the insert temperatures during profile production. Furthermore, actual production possibilities via additive manufacturing process in terms of maximum working dimensions have been taken into account at the insert design stage. To cope with all these requirements, several insert designs were generated incrementally implementing different suggestions. As a result, the design reported in Fig. 1a had a 1.5 mm diameter clockwise channel and simple inlet and outlet channels radially oriented (global dimensions are omitted for confidential reasons). An external face was made plane in order to fix the insert inside the housing thus avoiding an undesired motion/rotation during profile production.

Afterwards, a number of modifications to the first draft of the insert were implemented and evaluated. As an example, helix had to be turned counter clockwise in order to grant the

amount of space needed to place inlet, outlet channels and thermocouple hole, additionally considering the spatial constraints imposed by die geometry (Fig. 1b). A further design was provided with a final toroidal portion of the channel with 8 radial nitrogen outlets on the profile exit zone. This was thought to allow an inert gas covered zone where the profile flowing from the die exit reaches the highest temperature, thus avoiding profile oxidation (Fig. 2).

The last design was generated as a variation of the one proposed in Fig. 2, with a channel diameter of 3 mm (Fig. 3b) instead of 1.5 mm (Fig. 3a). A detailed comparison of the cross section of the two final designs shows that they not only differed in terms of cooling channel diameter (X quote) but also in terms of helix pitch (Y quote) and the axial position of the toroidal channel (Z quote). These modifications to the original design have been introduced with the double aim to not alter the structural integrity of the insert by maintaining the same void portion of the 1.5 mm version and to reduce the pressure drops within the channel.

As previously reported, the die concept has been developed with the idea to be decomposed in a ‘conventional part’ to be produced with conventional subtractive technologies and an ‘AM part’ to be printed by selective laser melting. In Fig. 3c is then reported one of the selected final versions of the insert design (1.5 mm diameter) mounted inside the conventional part of the die (steel housing).

### 3 Numerical modelling

Finite Element (FE) simulations of the extrusion process with the novel insert with conformal cooling channels (CCC) have been performed in order to properly predict the thermal field of the insert and of the profile and the level of stress induced by the in-service conditions. The global aim of the performed simulations was to guarantee an optimal tooling-set design able to maximize the process efficiency. In details, three stages

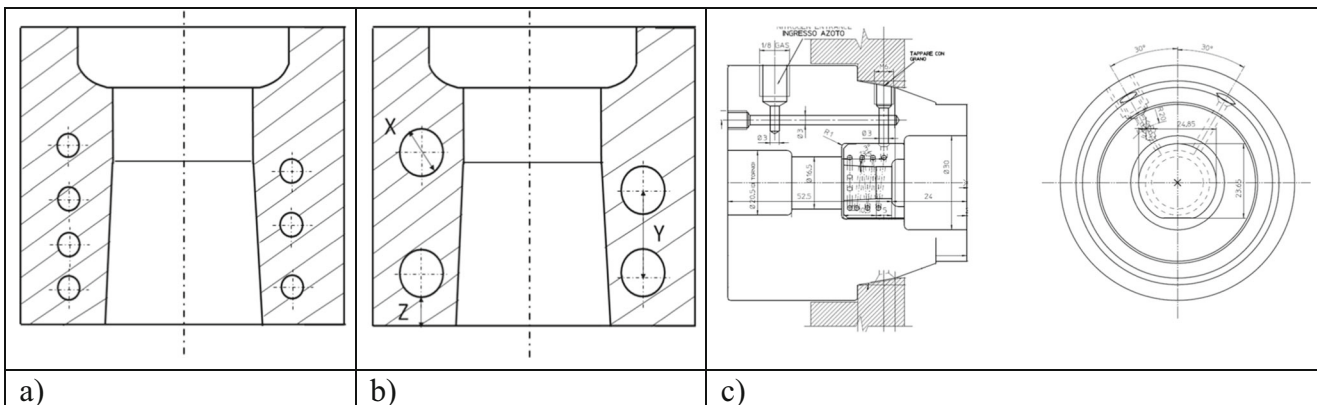


**Fig. 3** The final insert designs: 1.5 mm of cooling channel diameter **a** and 3 mm **b** and **c** the tooling set assembly (extrusion direction from right to left)

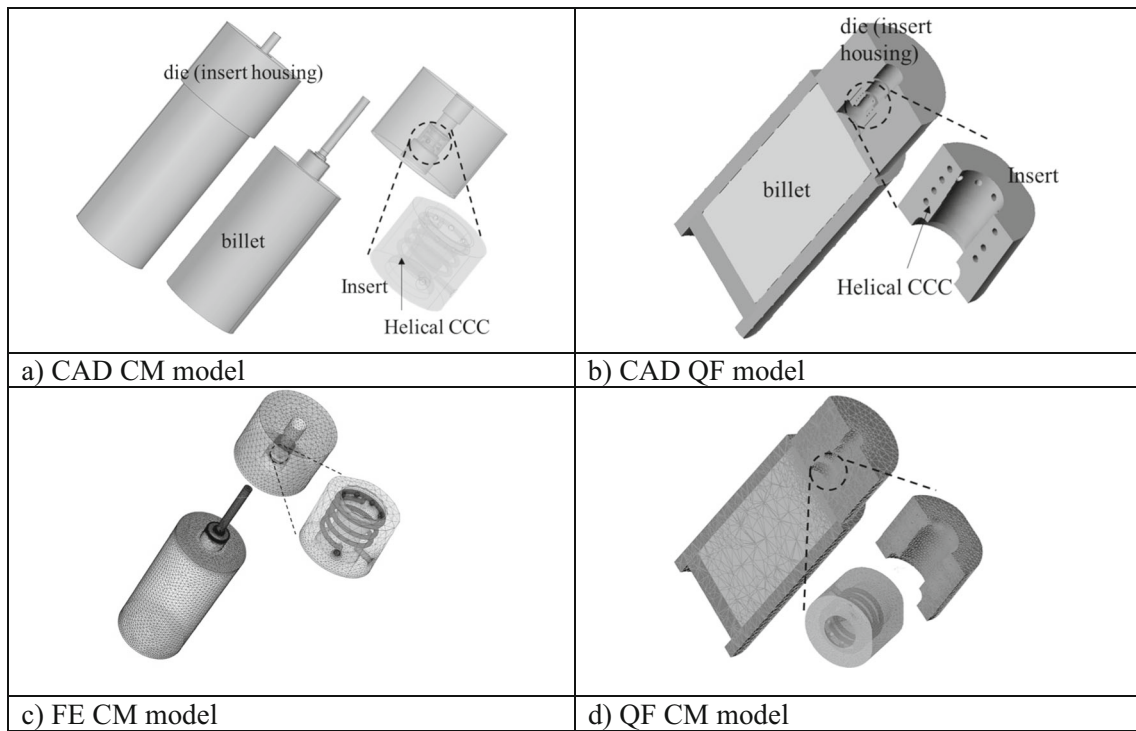


**Fig. 4** The CAD and FE models of the bar profile and of the insert with CCC of 1.5 mm diameter: a), c) COMSOL Multiphysics® (CM), b), d) Qform (QF)

of numerical modelling have been performed that are discussed in the following.

**3.1 FE model validation in uncooled conditions: QF vs CM**

For the FE simulations of the extrusion process, two codes were initially selected. The first code, Qform (QF), was selected since specifically dedicated to metal forming processes and for its wide literature validation

in the context of aluminum extrusion <http://qform3d.com/products/qformextrusion> [34–35]. It was therefore used to validate the numerical results achieved by the second code, COMSOL Multiphysics® (CM), a multi-purpose and multi-physics code selected due to its capability in modelling the die cooling by means of liquid nitrogen and in reducing the total computational time [32]. Qform is a Lagrangian FE code based on the flow-formulation in which the material is considered as an isotropic continuum while CM used a fluid-dynamic

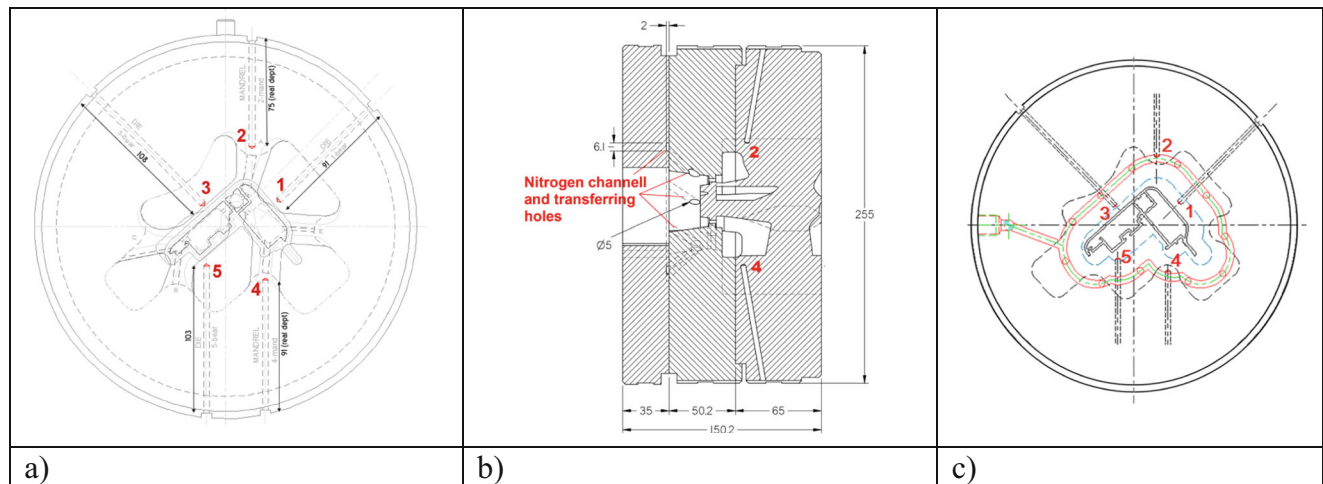
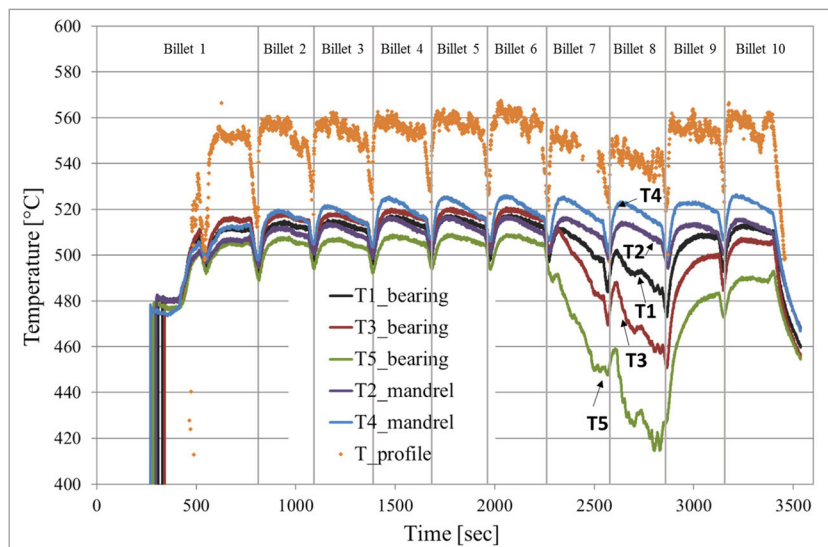


**Fig. 5** Thermocouples and nitrogen device in the mandrel, die, and backer. a Billet view. b Section view. c In plane view of profile, thermocouple location, and nitrogen cooling channel (billet view)

**Fig. 6** Temperature history recorded by thermocouples in the mandrel and in the die over the experimental testing time for the multi-hollow profile



approach to model the flow of the aluminum alloy during the extrusion [36, 37]. In Qform, the initial configuration of the billet was a cylinder of a certain length and diameter and both the ram and container were included in the model. In the CM code, the billet copied the steady-state configuration with the material already filling the die while the container and the ram were not included but their thermal and mechanical effects were taken into account by applying proper boundary conditions to the interfacing billet surfaces. The insert and the steel housing were merged in a single solid in order to reduce the computational time required to solve contact among bodies. The Fig. 4 a,b shows the initial CAD models of the 1.5 mm insert design for the two FE codes. The FE model of the extrusion process, considering the insert with CCC of 1.5 mm diameter, consisted of a total of 1,925,873 tetrahedral elements for the CM code (Fig. 4c) and an initial number of 359,593 tetrahedral elements for the QF code (Fig. 4d). The high number of elements used was generated by selecting a fine mesh option in the CM code and was due to the small channel diameter and

the curved channel surfaces to be approximated. For the QF code, the number of elements increased during the process simulation time thus reaching almost the same amount of the CM code for the same generated profile length.

In this preliminary validation phase, reasonable process parameters were selected to be used in the FE models accounting for a laboratory press that was supposed will be used in a future step of the work to perform the experimental trials on the inserts. In details, the initial billet, die and container temperatures were set to 480 °C, 490 °C and 400 °C respectively, while profile surfaces out of the bearings were set to the air temperature (25 °C). The initial billet length and diameter were set equal to 180 mm and 90 mm respectively. The aluminum-steel heat exchange coefficient was fixed to 11.000 W/m<sup>2</sup>K while a value of 3000 W/m<sup>2</sup>K was used at the outer die surfaces imposing an external temperature of 320 °C. At the tool/billet interfaces a sticking friction condition was generally imposed while on the profile surfaces, the slip friction condition was used. The ram speed was set to 5 mm/s, an average condition of industrial standards. The

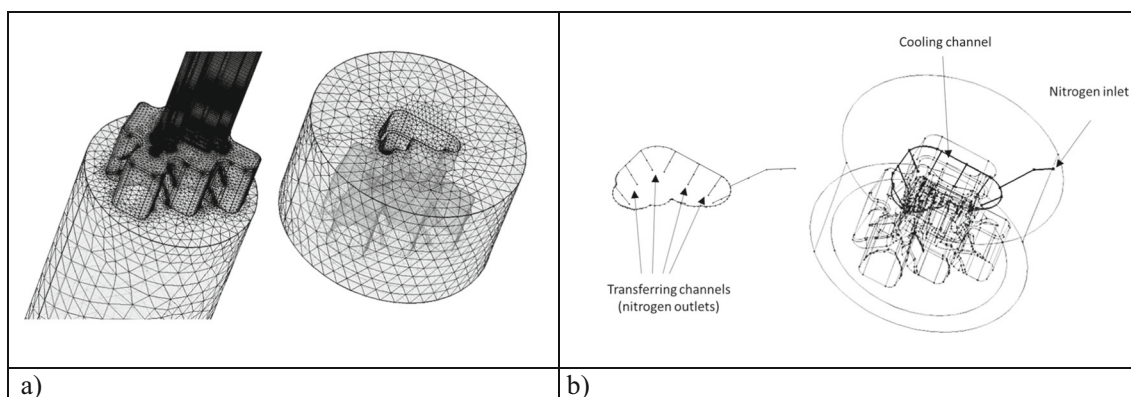


**Fig. 7** **a** The FE model of the multi-hollow profile generated in the CM code. **b** The 1D model of the nitrogen cooling channel

**Table 1** Fluid data of liquid nitrogen (isobaric data for  $P = 1$  bar)

Temperature (K)	Density (kg/m <sup>3</sup> )	Cv (J/g K)	Cp (J/g K)	Sound speed (m/s)	Viscosity (10 <sup>-3</sup> Pa s)	Thermal cond. (W/m K)	Phase
64.000	863.88	1.1706	2.0011	987.09	0.29527	0.17552	Liquid
66.000	855.58	1.1567	2.0048	966.70	0.26663	0.17093	Liquid
68.000	847.17	1.1431	2.0090	946.41	0.24177	0.16639	Liquid
70.000	838.64	1.1298	2.0140	926.18	0.22009	0.16190	Liquid
72.000	829.98	1.1169	2.0200	905.94	0.20111	0.15746	Liquid
74.000	821.18	1.1043	2.0269	885.66	0.18441	0.15307	Liquid
76.000	812.24	1.0921	2.0352	865.27	0.16968	0.14873	Liquid
77.244	806.59	1.0847	2.0410	852.53	0.16137	0.14605	Liquid

selected aluminum alloy was the AA6060 and the material model was the Sellars–Tegart inverse sine hyperbolic [38]:

$$\bar{\sigma} = \frac{1}{\alpha} \sinh^{-1} \left[ \frac{1}{A} \dot{\epsilon} \cdot \exp\left(\frac{Q}{RT}\right) \right]^{\frac{1}{n}} = \frac{1}{\alpha} \sinh^{-1} \left[ \left(\frac{Z}{A}\right) \right]^{\frac{1}{n}} \quad (1)$$

in which  $\bar{\sigma}$  is the flow stress,  $\dot{\epsilon}$  is the strain rate,  $Q$  the activation energy,  $R$  the gas constant,  $T$  the temperature and  $n$ ,  $A$  and  $\alpha$  material constants. This flow stress model was selected accounting for the fact that aluminum exhibits a viscoplastic behavior at elevated temperature. The coefficients used for the Sellars–Tegart constitutive law for AA6060 alloy (eq. 1) in the FE codes were  $n = 4.67$ ,  $Q = 161,000$  mol,  $A = 0.76301E11 s^{-1}$ ,  $R = 8.314$  J/(K $\cdot$ mol),  $\alpha = 0.035$  MPa<sup>-1</sup> with  $T$  expressed in  $^{\circ}$ K [39]. The AISI H13 steel was set for the die housing and the insert and the selected thermal and mechanical properties taken from codes' database.

In a preliminary validation phase of work, transient (time-dependent) simulations without nitrogen cooling were performed with QF and CM codes for the two insert designs (1.5 and 3 mm diameter) in order to compare output results in terms of temperature maps of the profile and of the insert and extrusion load for both insert designs. The stress state in the inserts was also evaluated by performing uncoupled mechanical analyses at the maximum process load.

### 3.2 FE model validation in cooled conditions with liquid nitrogen: Multi-hole profile

As second step of validation, since experimental data on the bar extrusion with the CCC inserts were not still available, the capability of the CM code to simulate the nitrogen cooling was preliminary validated against an industrial multi-hollow profile for which a dedicated experimental campaign was previously performed [11].

While in uncooled conditions the channels were modelled as 3D holes due to the requirement to compute the level of stress state in the insert, in the cooled simulation a 1D model was used. Indeed, the 3D modelling of the flow and heat transfer inside the cooling channels are computationally

expensive. An efficient alternative used to reduce the time required to solve the problem was the modelling of the flow and heat transfer in the cooling channels with 1D pipe flow equations, while still modelling the surrounding tooling set and billet in 3D. The non-isothermal pipe flow interface of the CM code, together with the CFD and heat transfer interfaces, were then used to model the nitrogen die cooling process. The equations describing the cooling channels are fully coupled by the multi-physics code to the heat transfer and CFD equations of the tooling set and aluminum part. The non-isothermal pipe flow was used to compute the temperature, velocity and pressure fields in pipes of different shapes. The parameters across the pipe were modelled as cross-section averaged quantities, which only varied along the length of the pipes and channels [40]. This way of modelling the cooling channels as 1D pipes was expected to offer excellent results in terms of computational time reduction with respect to a full 3D model.

For the multi-hole profile, the porthole die consisted of three parts, the mandrel, the die and the backer with the nitrogen cooling channel (Fig. 5a). Two K-thermocouples of 1 mm diameter and 1500 length were placed in the mandrel (thermocouples 2 and 4 in Fig. 5b) at 20 mm far from welding chamber wall to continuously monitor the temperature, while additional three K-thermocouples (1, 3 and 5 in Fig. 5a) were

**Table 2** Additional fluid data of liquid nitrogen ( $T = 77.355$  K and  $P = 1$  bar)

Property	Value
Normal boiling point (K)	77.355
Density (kg/m <sup>3</sup> )	806.59
Heat of vaporization (kJ/kg)	198.30
Specific heat (kJ/(kg K) $\times 10^{-1}$ )	20.40
Viscosity (10 <sup>-3</sup> Pa s)	157.90
Thermal conductivity (m W/(m K))	139.60
Critical temperature (K)	126.19
Critical pressure (bar)	33.96
Critical density (kg/m <sup>3</sup> )	313.30

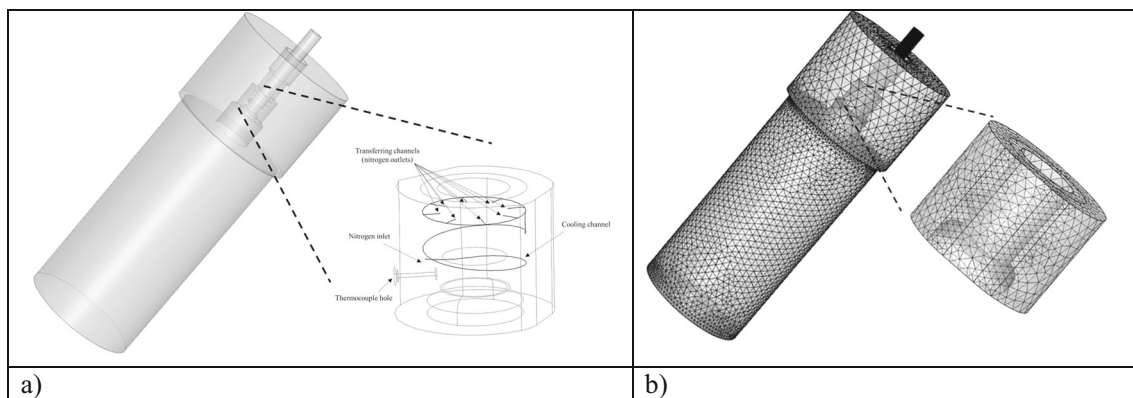


**Fig. 8** **a** The CAD model of the bar profile extrusion with the detail of the 1D model of cooling channel. **b** The corresponding FE model

used in order to monitor the die temperature. Thermocouples 1 and 3 were placed at 13 mm far from the bearings while thermocouple 5 at 16 mm. A nitrogen channel of 6.1 mm wide and 2 mm deep was manufactured in the backer (Fig. 5c) and connected to the profiles throughout holes of 5 mm diameter drilled in the die. As can be deduced by Fig. 5, cooling channel, milled in the third plate at the mating surface with the die, was located 35 mm far from bearings.

A pyrometer, placed out of the press, continuously recorded the profile exit temperature at a distance of 1660 mm out from the die face. Ten AA6060 billets were processed at 2.71 mm/s of ram speed during the trials. In details, three billets were initially extruded for homogenizing the temperature of the system without the use of the nitrogen, then three more billets were processed in the same conditions in order to evaluate the repeatability of the acquired data and finally four billets were extruded with the use of nitrogen die cooling under different flow rates (Fig. 6). Specifically, billets 7 and 8 were extruded with the nitrogen valve completely opened (100% of flow rate) while billet 9 and 10 with a reduced opening of 30% and 20% respectively. An Agilent multi-channel acquisition system was used connected to a laptop in order to record the thermocouples' data with 2 Hz of frequency. Additional experimental details can be found in [11].

In Fig. 7 is reported the FE model of the selected test case as generated in the CM code with the 1D model of cooling channel.

The initial temperatures set in the experimental plan were imposed in the numerical model. Specifically, a temperature of 480 °C was imposed to the die while 427 °C, 413 °C and 450 °C were those imposed to the container, the ram and the billet respectively and a ram speed of 2.71 mm/s was used in the model. The output conditions of billet 8, with the maximum nitrogen flow rate, (Fig. 6) were used as benchmark data to evaluate the code capability with 1D model of cooling channel to copy experimental results. A flow rate of 8 l/min was imposed to simulate a complete valve opening accounting for the nitrogen supplier indication of an average consumption of 0.2 l for each kilogram of aluminum. Material data of liquid nitrogen were taken from literature (Tables 1 and 2) [41] and a transient simulation performed.

### 3.3 FE model of the insert in cooled conditions with liquid nitrogen

In a third phase of the numerical work, the liquid nitrogen cooling was modelled in the CM code for the two insert designs. A total of 522,369 elements was used,

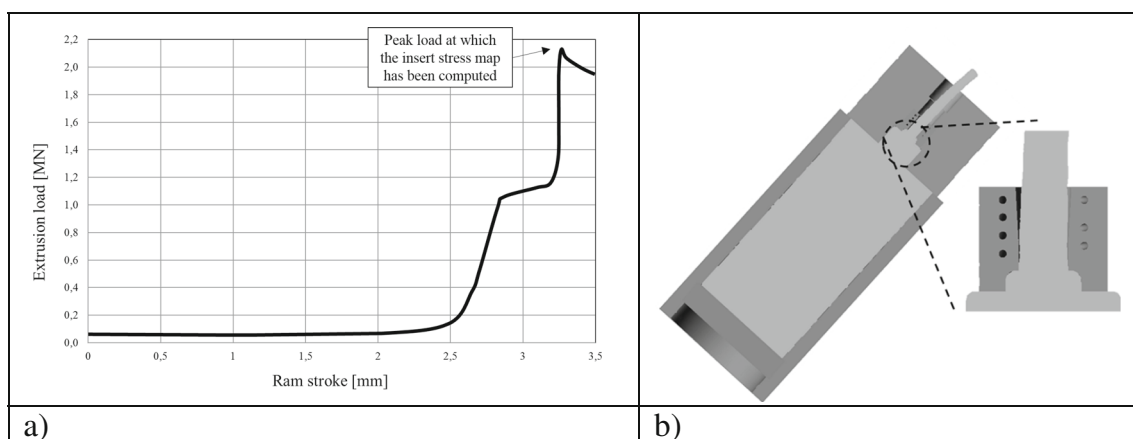


**Fig. 9** **a** Extrusion load history as predicted by the QF code for the 1.5 mm and 3 mm of CCC diameter inserts. **b** The simulated profile in the QF code



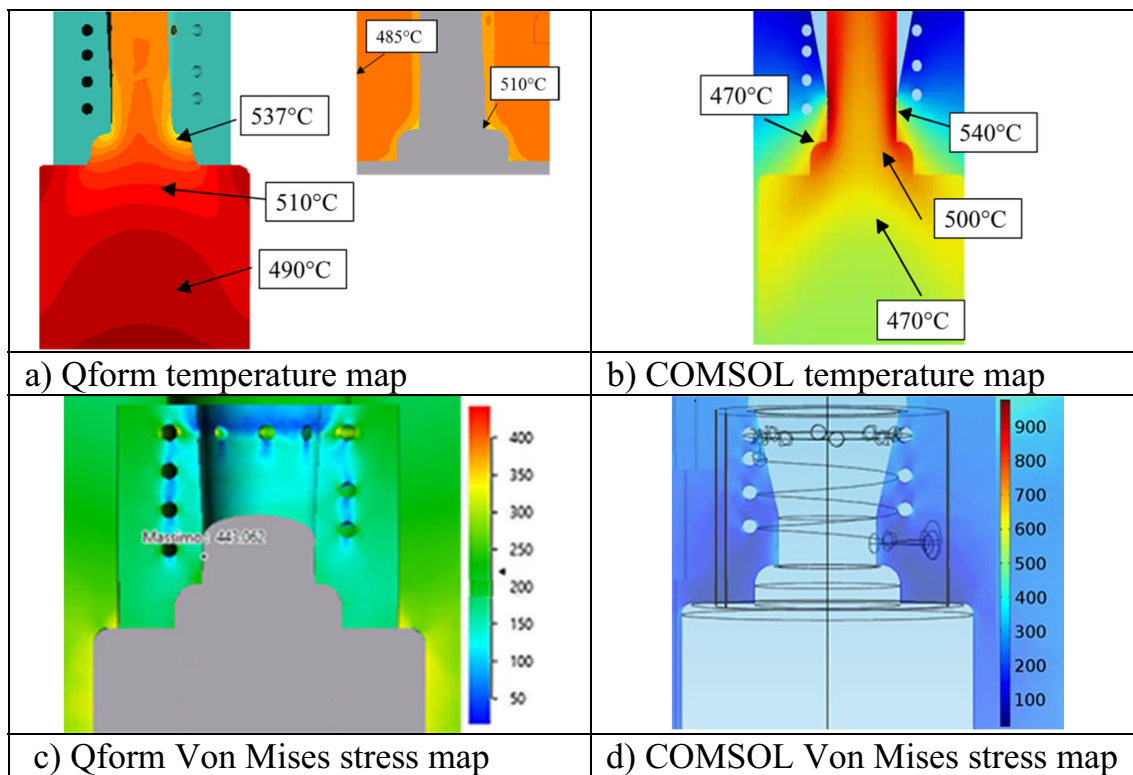


**Fig. 10** Temperature [°C] (a, b) and Von Mises stress [MPa] (c, d) maps as numerically predicted for the 1.5 mm CCC diameter configuration by the two codes

thus almost halved with respect to the model with a 3D cooling channel hole. Transient simulations were carried out in order to evaluate the thermal effect of the CCC in reducing the insert and profile exit temperatures. Cooling channels were modelled as a mono-dimensional pipe crossed by a non-isothermal fluid (Fig. 8) using the same nitrogen properties previously tested for the multi-hole profile.

The same extrusion parameters used in the first validation of the CM insert model in uncooled conditions were used. Results has been assessed in terms of peak extrusion load and temperature maps in the die (housing and insert) as well as in the profile. In addition, the 3 mm insert was further tested at three levels of ram speed (2.5, 5 and 10 mm/s) and compared to the corresponding results achieved in uncooled conditions with the aim to check the nitrogen cooling effect on the production rate.

## 4 Numerical results

### 4.1 FE model validation in uncooled conditions: QF vs CM

As first result, the Qform (QF) and the COMSOL Multiphysics® (CM) codes were compared in uncooled conditions. The stress state of the two insert designs was evaluated, and for the QF code, it was calculated at the value of the ram stroke corresponding to the maximum extrusion load (Figs. 9 and 10c).

No significant differences were observed for the two insert designs so that a unique load history has been reported in Fig. 9a. The typical load history trend can be observed with the first 2.5 mm of stroke used to approach the ram to the billet. Then the load increased between 2.5 and 3.2 mm of stroke due to the billet upsetting within the container followed

**Table 3** The QF/CM output results comparisons for the 1.5 mm of cooling channel diameter insert

	Qform (QF)	COMSOL (CM)	% Error
Peak extrusion load	2.14 MN	2.15 MN	0.47
Peak Von Mises stress in the insert	443 MPa	450 MPa	1.58
Average Von Mises stress in the insert	150 MPa	158 MPa	5.33
Peak exit profile temperature	537 °C	540 °C	0.56
Average temperature of the insert	405 °C	400 °C	1.23

**Table 4** The QF/CM output results comparisons for the 3 mm of cooling channel diameter insert

	Qform (QF)	COMSOL (CM)	% Error
Peak extrusion load	2.16 MN	2.17 MN	0.5
Peak Von Mises stress in the insert	818 MPa	818 MPa	0.0
Average Von Mises stress in the insert	300 MPa	302 MPa	0.7
Peak exit profile temperature	540 °C	560 °C	3.7
Average temperature of the insert	410 °C	422 °C	2.9

by a steep rising due to the work required to deform the billet and to overcome friction till reaching the maximum load when the material started to flow out of the insert orifice. Due to the high computational time required by the Lagrangian code, only few millimeters of profile were simulated (Fig. 9b). A detailed comparison of the results achieved by the two codes for the 1.5 and 3 mm CCC diameter inserts is reported in Tables 3 and 4.

As can be seen, a very good agreement was achieved between the output results of the two codes, both in terms of thermal and mechanical loads. The peak % error was less than 6% for the average Von Mises stress for the 1.5 mm insert design, with an average percentage error of 1.7%.

In Fig. 10 are reported, as an example, the temperature and the Von Mises stress maps of the 1.5 mm CCC insert design as predicted by the two codes.

It can be further observed that the level of the predicted insert stress remains in each case under the yielding point, which suggests a proper resistance of the inserts to the in-service loads in uncooled conditions.

#### 4.2 FE model validation in cooled conditions with liquid nitrogen: Multi-hole profile

The experimental cooled conditions of the multi-hole profile were simulated by means of the 1D model of the channels. As previously explained, the experimental output results of billet 8 (Fig. 6), with the peak nitrogen flow rate, were used as benchmark data to evaluate the numerical predictions of the CM code. In Table 5 are reported the experimental and numerical results in terms of temperatures in the thermocouples and on the profile.

Higher discrepancies were found for the thermocouples 2 and 4 placed in the mandrel for which errors of 5% and 7.7%

were found respectively. In the die locations experimental-numerical errors were significantly lower achieving, for thermocouples 1 and 5, a perfect matching. In addition, a good agreement was also obtained in terms of extrusion load with an experimental value of 19.8 MN and a numerical prediction of 19.5 MN. The experimental-numerical difference in the profile exit temperature can be due to the fact that the effect of the nitrogen exiting the cooling channels was not modelled, while in the experiment it directly cooled the profile. As an additional consideration, Fig. 11 clearly evidences the asymmetric cooling effect of the nitrogen, more pronounced nearby the inlet of the channel (blue area) than on the opposite side. It then clearly emerges that the FE model with 1D cooling channel was able to accurately predict the level and the distribution of temperatures achieved due to the nitrogen cooling thus supporting its use for the assessment of the insert thermal functionality.

#### 4.3 FE model of the insert in cooled conditions with liquid nitrogen

At this stage of the work, the 1D model of the cooling channel was used to simulate the inserts cooling with liquid nitrogen. Transient simulations were performed by setting an end-time of 60 s in order to achieve a steady-state thermal condition. As first result, the thermal gradient induced by the coupling of the extrusion process with the nitrogen flowing into the 3 mm cooling channel insert was compared to that achieved in the uncooled condition at the same ram speed (5 mm/s) (Fig. 12).

A detailed analysis of Fig. 12 clearly shows the effect of the nitrogen cooling. For the insert, it can be observed a colder region (blue zones) corresponding to the helical path of the channel and to the exit from the bearings. However, in the forming zone of the insert, in which the temperature was

**Table 5** Numerical output predictions of the transient analyses performed with the CM code compared to experimental data for cooled conditions with liquid nitrogen of the multi-hole profile

	T1	T2	T3	T4	T5	Profile exit T°
Experimental	490 °C	505 °C	460 °C	520 °C	430 °C	540 °C
Numerical	490 °C	480 °C	450 °C	480 °C	430 °C	550 °C
% Error	0.0	5.0	2.2	7.7	0.0	1.9

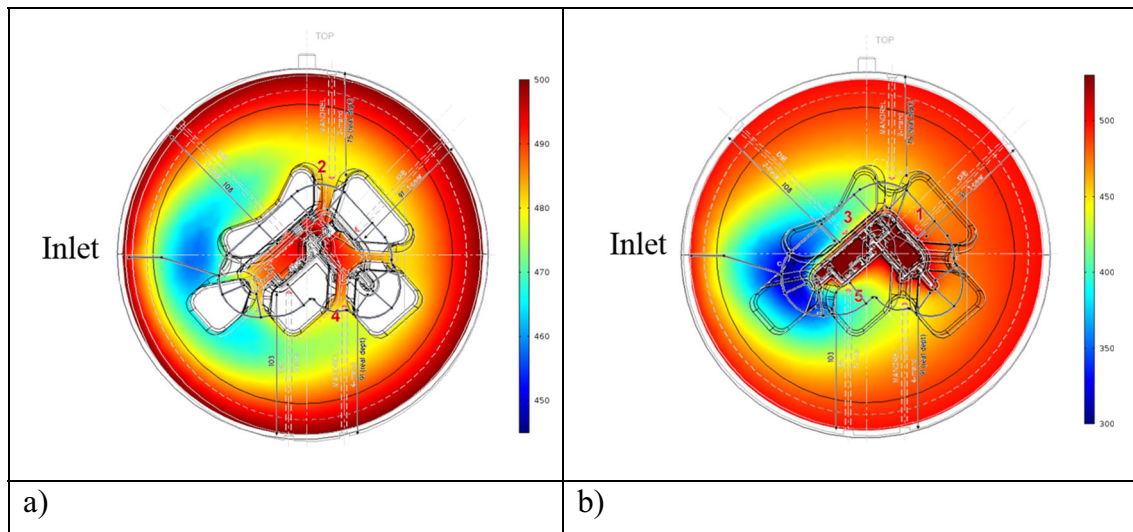


**Fig. 11** Temperature maps of the tooling set as numerically predicted by COMSOL Multiphysics® code in cooled conditions with liquid nitrogen. The experimental thermocouple placement is also visible: cross sections of **a** mandrel locations and **b** die locations

required to remains high in order to deform the material and generate the profile, the temperature was only slightly reduced of a 2% (from 500 °C to 490 °C) thus confirming a properly defined position of the cooling channel. The average insert temperature dropped from 453 °C of the uncooled condition to 210 °C of the cooled state suggesting an important awaited increase of the insert lifetime. The temperature of the forming material in the bearings was decreased of 20 °C (from 560 to 540 °C) reducing the risk of profile defect generation. A temperature drop of 30 °C (from 380 to 350 °C) was achieved for the housing die during the process ascribable not only to the nitrogen cooling but also to the heat exchange with the adjoining tools.

In Fig. 13 are reported the comparisons of the thermal history of the two insert designs in terms of peak profile exit temperature, peak temperature of the profile in the forming zone (in contact with the bearings) and average temperature of the insert.

Starting from the initial imposed values of the billet (480 °C) and the insert (490 °C), the peak temperature in the forming zone and of the exiting profile initially increased in the first 2 s of simulation due to the prevailing effect of the heat generated for deforming the billet and overcome the friction on that removed by liquid nitrogen within the channel (Fig. 13a). After that, the temperatures dramatically dropped owing to the nitrogen action with a significant effect, as previously observed, on the average temperature value of the insert. The peak exit profile temperature was lower than that of the forming zone due to the heat exchange with the surrounding air supposed at room temperature. If the two insert designs are compared, it emerges that no substantial differences can be found in terms of peak temperature in the profile and in the forming zone while a not negligible deviation is observed for the average temperature in the insert, with the 1.5 mm design showing a lower value. This thermal behavior can be justified by considering the insert geometry that, for the 1.5 mm design, is marked by a reduced

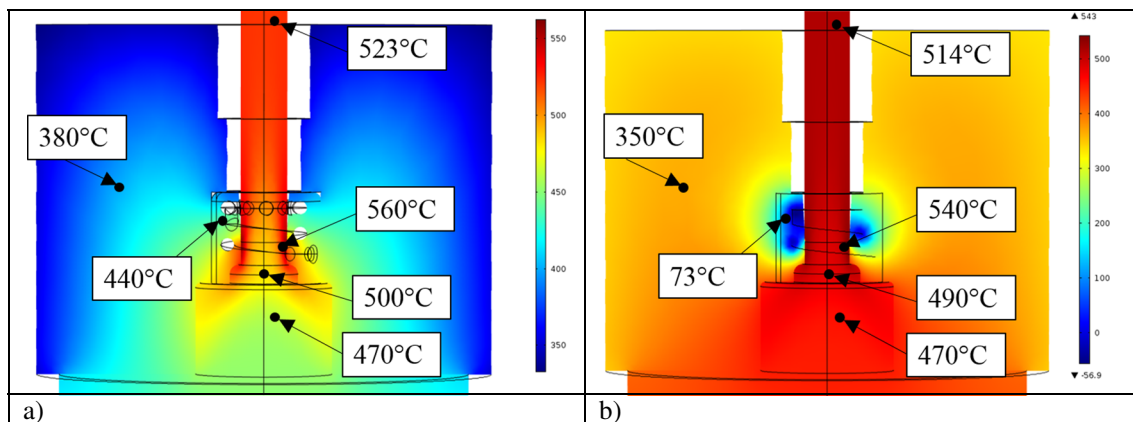


**Fig. 12** The simulated thermal gradient induced in the 3 mm CCC diameter insert design with a 5 mm/s of ram speed. **a** Uncooled condition. **b** Cooled condition with liquid nitrogen

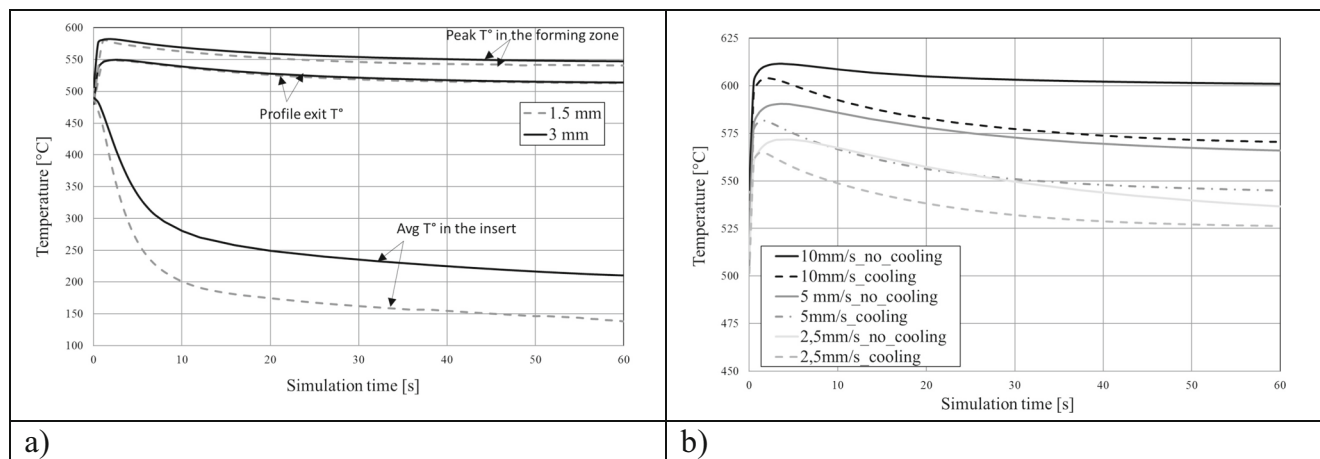


**Fig. 13** **a** Comparison of the 1.5 and 3 mm CCC diameter insert designs in terms of peak temperature history in the profile and in the forming zone and average temperature in the insert. **b** peak temperature history in the

forming zone for the 3 mm insert design at three levels of ram speed for cooled and uncooled conditions

helical pitch than that of the 3 mm one thus having a longer cooling path (Fig. 3a,b). As an additional consideration, it was numerically predicted a very high inlet pressure required to guarantee a nitrogen flow rate of 1 l/min for the 1.5 mm insert design (4 bar), while a more reasonable data was attained for the 3 mm design (1.1 bar) [9].

As last step of the work, the cooled and uncooled conditions were numerically tested at three levels of extrusion speed, i.e., 2.5, 5 and 10 mm/s for the 3 mm of CCC diameter insert. Results are reported in Fig. 13b in terms of peak temperature history in the forming zone. It can be observed that the same level of temperature reached at 5 mm/s was achieved by doubling the ram speed (10 mm/s) if the nitrogen cooling with the designed CCC was used, thus allowing a significant increasing of the production rate. Of course, the numerically tested condition at 10 mm/s without cooling has to be considered not realistic since generating a profile exit temperature of 610 °C, next to the aluminum melting point, but it was included in order to get a comprehensive quantitative estimation of the gain achievable in terms of production rate with the use of nitrogen cooling. The same considerations can be made for the lower ram speed of 2.5 mm/s with the final value of temperature in uncooled conditions approaching that of the cooled insert at 5 mm/s.

## 5 SLM insert manufacturing

The results of the previous performed numerical activities allowed to assess the inserts thermal and mechanical

performances. The two geometries were then produced via SLM (Selective Laser Melting) process using a SISMA Industries MYSINT 100 LM. The machine had a working chamber dimension of 100 mm in diameter and 160 mm in height, delivering a maximum laser power of 150 W with a laser spot of 50  $\mu\text{m}$ . Commercial SLM grade H13 steel powder was provided by LPW Europe and its chemical composition is reported in Table 6.

The selected process parameters for inserts production (Table 7) were evaluated and tuned in former internal research activities related to the production of “thin” or “average” wall components.

In the first production batch, three dies inserts with 1.5 mm CCC diameter, plus another “thick-walled”, were placed on a C40 cold platform (Fig. 14b). The total printing time was approximately 18 h. As main result, at the end of the SLM process, all of the components resulted severely cracked (Fig. 14b,c). The cracks followed a “periodical” distribution, which means that a new crack originated on the outer surface at almost the same distance from the previous ones, along the component axis direction, corresponding to the growth direction (Fig. 14b). Moreover the cracks originated from the outer surface going towards the inner cooling channel (Fig. 14c). This behavior was clearly caused by thermally induced stress during the production phases. It was observed that, taking into account a single component, more than 1 min was necessary for the laser beam to melt the next powder layer. This could cause harsh thermal gradients within the components thus leading to severe stresses. In order to solve this issue, it was

**Table 6** H13 steel average composition

C	Cr	Mn	Mo	Ni	Si	V	Fe
0.32–0.45	4.75–5.50	0.2–0.5	1.10–1.75	$\leq 0.3$	0.8–1.2	0.8–1.2	Balance

**Table 7** SLM process parameters selected for inserts production

Fluency ( $J/mm^3$ )	Power (W)	Speed (mm/s)	Hatch distance (mm)	Layer depth ( $\mu m$ )
143	100	700	0,05	20

decided to produce on a new platform just two inserts, thus allowing a dramatic decrease of waiting time from one to another layer melting. As first attempt, two 1.5 mm inserts design were printed (Fig. 15a). This probably resulted in a reduced thermal gradient within the component, higher average temperature during its production and less severe thermally induced stresses. As can be seen in Fig. 15b, the components produced in such a way resulted completely crack-free and geometrically compliant to the formerly developed design. This demonstrated that limiting the number of components on the platform during their growth likely resulted in milder residual stresses thus no crack appeared, as can also be checked by the visual inspection of a sectioned insert (Fig. 15c).

At the end of the preliminary experimental phase, a total of 8 final inserts were manufactured, 4 for each insert design. Their hardness in the “as produced” condition was of  $48 \pm 2$  HRC. Optical microscopy evaluation showed the typical microstructure coming from SLM process with its “banded” appearance coming from melt pools solidification (Fig. 16a).

A stress relief treatment (5 Hours at  $350^\circ C$ , still on the C40 platform) was carried out and components hardness lowered to  $43 \pm 2$  HRC. After the stress relief, the components were detached from the platforms and machined via turning on the outer surfaces.

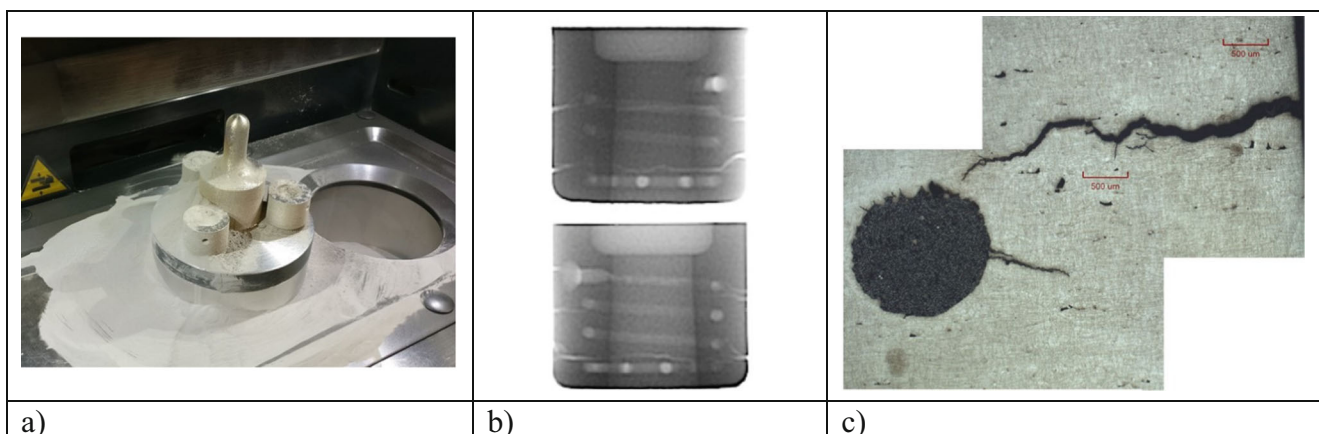
The final heat treatment consisted in an austenitization at  $1020^\circ C$ , gas quenching using forced pressure nitrogen, first tempering at  $550^\circ C$  and second tempering at  $585^\circ C$  resulting in a final hardness of  $\sim 45$  HRC. The microstructure analysis after heat treatment showed a much more uniform phase distribution: no melt pool boundary segregations were visible

any more (Fig. 16b). The average area fraction of pore within two cut components was of  $0.75 \pm 0.44\%$ .

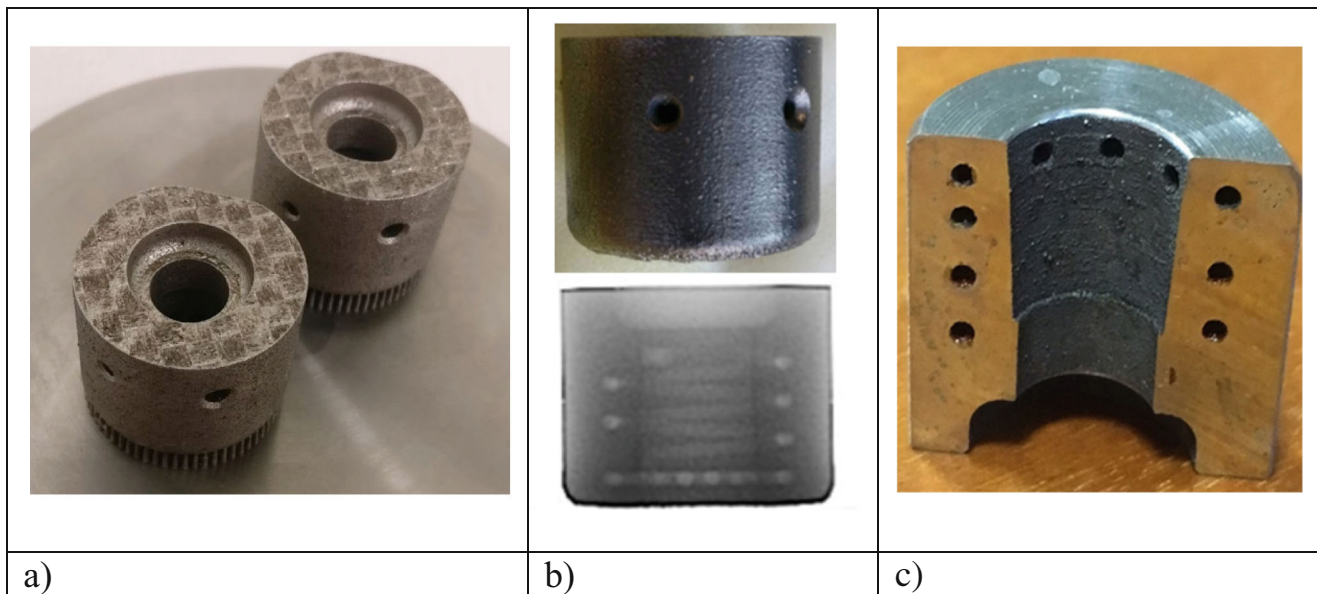
After final EDM machining of the die insert bore and superfinishing, two die inserts (one with 3 mm in diameter and the other one with 1.5 mm of cooling channels diameter) were mounted into the die holders, as can be seen in Fig. 17. The steel housing has been designed and manufactured by the die maker Almax Mori Srl (TN), Italy. The cooling channels system lack of obstruction was tested by purging compressed air. No assembly issue was highlighted. Experimental trials of the manufactured SLM inserts are now under planning and will be carried out in a near future in order to both verify the insert thermal functionality and the FE simulations performances.

## 6 Conclusions

In the present work, a novel thermally controlled extrusion insert with Conformal Cooling Channels (CCC) for the extrusion of a bar profile has been designed and additively manufactured by means of the Selective Laser Melting (SLM) process. After a preliminary design stage of the insert, a comprehensive numerical investigation has been performed in order to check the selected insert designs thermal and mechanical performances in uncooled and cooled conditions. To this aim, a novel FE model of the extrusion process coupled with nitrogen cooling, in which the channel was modelled as 1D pipe, has been developed in the COMSOL Multiphysics® code and conveniently validated. The main outcomes of the work can be summarized as follow:



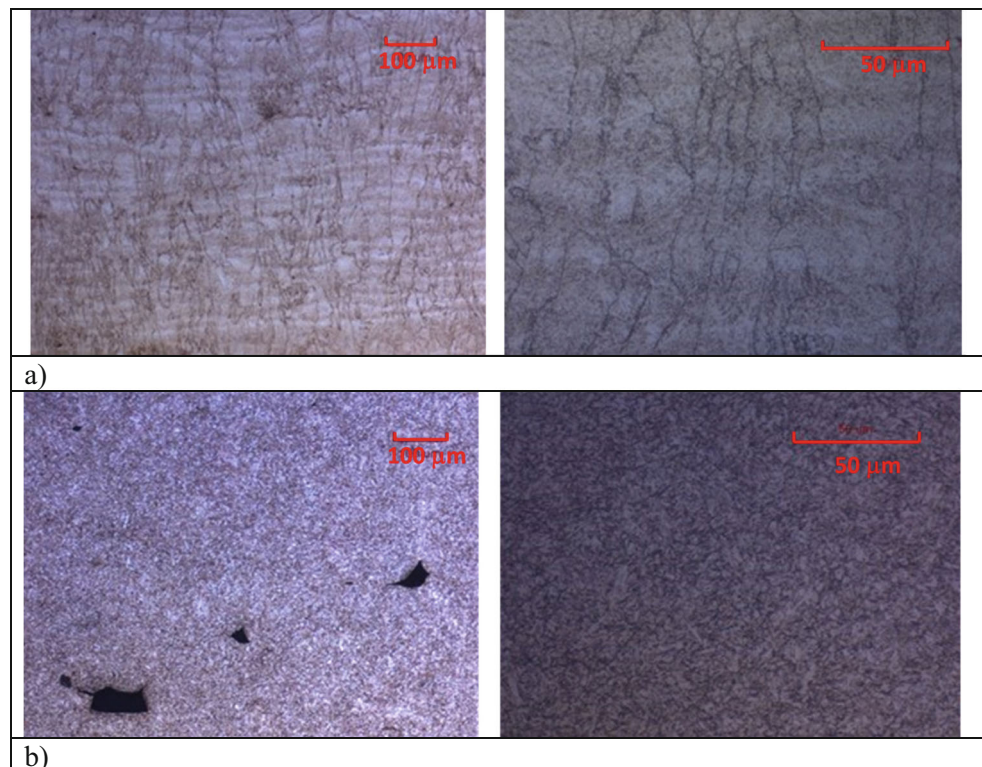
**Fig. 14** **a** First inserts production batch with four “thick-walled” components grown onto a C40 cold platform. **b** X-ray analysis of one of the printed inserts. **c** Magnification of an optical micrograph in the region of cooling channel section (cracks are clearly visible)



**Fig. 15** **a** Second inserts production batch (inserts with CCC of 1.5 mm diameter). **b** Picture (top) and X-ray analysis (bottom) of a printed insert. **c** Longitudinal section of the insert without evident cracks

- The COMSOL Multiphysics®-Qform comparison for the uncooled conditions of the bar profile showed a good matching of the results with a peak percentage discrepancy of less than 6% thus confirming the COMSOL code capability to accurately simulate an extrusion process.
- A good experimental-numerical predictions was achieved for the multi-hole profile with COMSOL Multiphysics®
- by means of the 1D model of liquid nitrogen channel with a peak error of 7.7% in the temperature estimation thus suggesting the ability of the developed model to accurately simulate the extrusion process in liquid nitrogen cooled conditions.
- In the forming zone of the inserts, in which the temperature needs to remain high in order to easily deform the

**Fig. 16** **a**) Microstructure in “as produced” condition; **b**) Microstructure after the final heat treatment



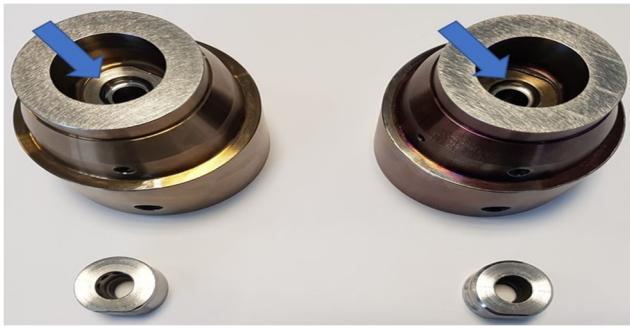


**Figure 17** Two inserts mounted into holding die (by Almax Mori Srl, Italy): (top) holding die and (bottom) inserts before assembly.

material, it was only slightly reduced by the liquid nitrogen cooling of a 2% thus confirming a properly defined position of the cooling channel.

- The transient simulations performed for the bar profile at different extrusion speed showed the potential of the insert with conformal cooling channels to allow almost a doubling of the production rate without coming to critical working temperatures.
- The Selective Laser Melting (SLM) process was able to properly manufacture a complex 3D part made of H13 hot work tool steel resulting in free of cracks and dense components

The performed simulations and the achieved results thus suggest a proper insert thermal functionality with the selected design and process parameters allowing to double the ram speed without coming to critical temperature ranges both for the profile and the insert. This should then guarantee an increased production rate, a defect-free profile production and an extended insert lifetime. In addition, even if these are preliminary investigations requiring further insights, to the best author's knowledge, the performed simulations represent the first attempt to simulate the complex coupling of nitrogen cooling system with thermo-structural analyses of the extrusion process. Once experimentally validated, the generated model of the insert could be used to exploit the performances of variable channel aspect ratio and fluid flow in order to optimize the insert thermal efficiency and structural integrity.

**Acknowledgments** Authors would like to thank Eng. Riccardo Pelaccia for the support in setting numerical simulations. This publication was produced with the contribution of the Ministry of Foreign Affairs and International Cooperation.

## References

1. Saha PK (2000) Aluminum extrusion technology. ASM Int. Materials Par, OH
2. Matienzo LJ, Holub KJ, Vandatta W (1982) Investigation on surface defects produced during the extrusion of some aluminum alloys. *Appl Surf Sci* 15:307–320
3. Parson N.C, Jowett C.W., Pelow C.V., Fraser WC (1996) Surface defects on 6xxx alloy extrusions. *Proceedings of the 6th International Extrusion Technology Seminar*, 1:57–68
4. Arif AF, Sheikh AK, Qamar SZ, Raza MK, Al-Fuhaid KM (2002) Product defect in aluminum extrusion and their impact on operational cost. *Proceedings of the 6th Saudi Engineering Conference*. KFUPM, Dhahran, 5:137–154
5. Klaus A (2016) How to benefit from isothermal extrusion. *Proceedings of the 11th International Extrusion Technology Seminar*, vol 2, pp 215–220
6. Benedyk J (2008) The evolution of the smart container: achieving isothermal control in extrusion. *Light Met Age*, August 2008:40–47
7. Zasadziński J, Libura W, Richert J (2004) Fundamentals of advanced aluminum extrusion processes. *Proceedings of the 8th International Extrusion Technology Seminar*, vol 2, pp 391–397
8. Holker R, Jager A, Khalifa NB, Tekkaya AE (2012) New concepts for cooling of extrusion dies manufactured by rapid tooling. *Key Eng Mater* 491:223–232
9. Donati L, Segatori A, Reggiani B, Tomesani L, Bevilacqua Fazzini PA (2012) Effect of liquid nitrogen die cooling on extrusion process conditions. *Key Eng Mater* 491:215–222
10. Ward TJ, Kelly RM, Jones GA, Heffron JF (1984) Effects of nitrogen - liquid and gaseous - on aluminum extrusion. *J Miner Met Mater Soc* 36(12):29–33
11. Stratton P (2008) Raising productivity of aluminium extrusion with nitrogen. *Intl Heat Treat Surf Eng* 2(3–4):105–108
12. Ciuffini A.F, Barella S., Di Cecca C., Gruttadauria A., Mapelli C., Merello L., Mainetti G., Bertolotti M
13. Mazur M., Leary M., McMillan M., Elambasseril J., Brandt M (2016) SLM additive manufacture of H13 tool steel with conformal cooling and structural lattices. *Rapid Prototyp J* 22(3):504–518
14. Mazur M, Brincat P, Leary M, Brandt M (2017) Numerical and experimental evaluation of a conformally cooled H13 steel injection mould manufactured with selective laser melting. *Int J Adv Manuf Technol* 93:881–900
15. Wu T, Jahan SA, Kumaar P, Tovar A, El-Mounayri H, Zhang Y, Zhang J, Acheson D, Brand K, Nalim R (2015) A framework for optimizing the design of injection molds with conformal cooling for additive manufacturing. *Procedia Manuf* 1:404–415
16. Km A, Km Y (2013) Conformal cooling channel design and CAE simulation for rapid blow mould. *Int J Adv Manuf Technol* 66:311–324
17. Muller B, Gebauer M, Hund R, Malek R, Gerth N (2009) Metal additive manufacturing for tooling applications – laser beam melting technology increases efficiency of dies and molds. In the Proc. of the metal additive manufacturing conference, 20th -21st November 2014, Wien
18. Schwam D (2015) Additive manufacturing for die casting applications. *Die Casting congress & exposition – NADCA (North 800 American Die Casting Association)*, 5-7 October 2015, Indianapolis, United States
19. Armillotta A, Baraggi R, Fasoli S (2014). SLM tooling for die casting with conformal cooling channels. *Int J Adv Manuf Technol* 71(1-4):573–583
20. Holker R, Jager A, Khalifa NB, Tekkaya AE (2013) Controlling heat balance in hot aluminum extrusion by additive manufactured extrusion dies with conformal cooling channels. *Int J Precis Eng Manuf* 14(8):1487–1493
21. Holker R, Tekkaya AE (2016) Advancements in the manufacturing of dies for hot aluminum extrusion with conformal cooling channels. *Int J Adv Manuf Technol* 83:1209–1220
22. Yan JJ, Zheng DL, Li HX, Jia X, Sun JF, Li YL, Qian M, Yan M (2017) Selective laser melting of H13: microstructure and residual stress. *J Mater Sci* 52:12476–12485

23. Safka J, Ackermann M, Volesky L (2016) Structural properties of H13 tool steel parts produced with use of selective laser melting technology. *J Phys* 709:012004
24. Holzweissig MJ, Taube A, Brenne F, Schaper M, Niendor T (2015) Microstructural characterization and mechanical performance of hot work tool steel processed by selective laser melting. *Metall Mater Trans C* 6B:545
25. Reggiani B, Donati L (2018) Additive manufacturing for extrusion dies. *Light Met Age*:10–17
26. Donati L, Tomesani L (2005) The effect of die design on the production and seam weld quality of extruded aluminum profiles. *J Mater Process Technol* 164–165:1025–1031
27. Reggiani B, Donati L (2017) ICEB - International Conference on Extrusion and Benchmark. *Light Met Age*:52–60
28. He Z, Wang H, Wang M, Li G (2012) Simulation of extrusion process of complicated aluminium profile and die trial. *Trans Nonferrous Metals Soc China* 22(7):1732–1737
29. Zhang C, Zhao G, Chen Z, Chen H, Kou F (2012) Effect of extrusion stem speed on extrusion process for a hollow aluminum profile. *Mater Sci Eng B* 177(19):1691–1697
30. Reggiani B, Segatori A, Donati L, Tomesani L (2013) Prediction of charge welds in hollow profiles extrusion by FEM simulations and experimental validation. *Int J Adv Manuf Technol* 69(5–8):1855–1872
31. Schikorra M, Donati L, Tomesani L, Kleiner M (2007) The role of friction in the extrusion of AA6060 aluminum alloy, process analysis and monitoring. *J Mater Process Technol* 191:288–292
32. Reggiani B, Donati L, Tomesani L (2017) Multi-goal optimization of industrial extrusion dies by means of meta-models. *Int J Adv Manuf Technol* 88(9–12):3281–3293
33. Shinde MS, Ashtankar KM (2017) Additive manufacturing-assisted conformal cooling channels in mold manufacturing processes. *Adv Mech Eng* 9(5):1–14
34. Li XR, Fang WL, Tang D, Qiao Y, Sun YL, Li DY (2017) Numerical simulation on hot extrusion forming of aluminum alloy micro-multiport profile. *J Plasticity Eng* 24(5):1–6
35. Bandini C, Reggiani B, Donati L, Tomesani L (2017) Code validation and development of user routines for microstructural prediction with Qform. *Mater Today* 2(10):4904–4914
36. Reggiani B, Donati L, Tomesani L (2010) Evaluation of process speed effect in aluminium extrusion by experiment and simulations. In: *Proc. of the TMS 2010 139th Annual Meeting & Exhibition*, February, 14–18, vol 1. Washington State Convention Center, Seattle, pp 65–70
37. Irgens F (2014) *Rheology and non-Newtonian fluids* (ebook). Springer International Publishing Switzerland, first edition
38. Sellars CM, Tegart WJMG (1972) Hot workability. *Int Metall Rev* 17(1):1–24
39. Verlinden B, Suhadi A, Delaey L (1993) A generalized constitutive equation for an AA6060 aluminum alloy. *Scr Metall Mater* 28(11):1441–1446
40. COMSOL® Multiphysics (Version 5.3a). Modelling software. <https://www.comsol.it>
41. Lemmon EW (2003) Thermophysical properties of fluid systems. NIST Chemistry WebBook
42. Akaret R (1980) Das verhalten der Strangpresse als Regelstrecke. *Metall* 34(8):737–741

**Publisher's note** Springer Nature remains neutral with regard to jurisdictional claims in published maps and institutional affiliations.